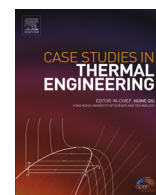


Contents lists available at ScienceDirect

Case Studies in Thermal Engineering

journal homepage: www.elsevier.com/locate/csite

Research on heat transfer characteristic for hot oil spraying heating process in crude oil tank

Jian Zhao^{*}, Lixin Wei, Hang Dong, Fengrong Liu

Key Laboratory of Enhance Oil and Gas Recovery of Educational Ministry, Northeast Petroleum University, Daqing, PR China

ARTICLE INFO

Article history:

Received 15 December 2015

Received in revised form

5 April 2016

Accepted 6 April 2016

Available online 11 April 2016

Keywords:

Numerical simulation

Heat transfer

Buoyancy jet flow

Hot oil spraying

Crude oil

ABSTRACT

The finite volume method and standard $k - \varepsilon$ turbulence model are used to numerically investigate the heat transfer features of crude oil inside the floating roof tank under the hot oil spraying heating mode. The results indicate that this heat transfer process has the essential features of the thermal buoyancy jet flow. The jet flow is divided into the strong buoyancy, weak buoyancy and common buoyancy process according to Froude number of the jet flow. Bigger Froude number of the jet flow indicates stronger heat exchange strength and more uniform distribution of oil temperature. Smaller Froude number indicates stronger buoyancy, weaker heat exchange strength and more obvious hierarchical distribution feature of the oil temperature inside the tank. Two indices (efficiency and uniformity) are introduced and examined which could be of practical usage. According to the simulated result, higher nozzle speed and proper spraying temperature which results in a larger Froude number can achieve better heating effect by taking two previous indices as evaluation criterion. For the practical engineering usage, the spraying temperature and nozzle speed should be adjusted synchronously based on Froude number.

© 2016 The Authors. Published by Elsevier Ltd. This is an open access article under the CC BY-NC-ND license (<http://creativecommons.org/licenses/by-nc-nd/4.0/>).

1. Introduction

In the northeast of china, the air temperature in winter can reduced to $-30\text{ }^{\circ}\text{C}$ which is much lower than the condensation point of crude oil in that region, leading the safety storage of oil be more difficult. In order to increase the fluidity of oil, keeping it at a high temperature by heating is the most common method. Comparing to the traditional heating mode of heating tube system, the hot oil spraying heating mode has a higher heat exchange efficiency and is extensively applied in the crude oil tank in recent years. For the hot oil spraying heating mode, the oil in the tank becomes the heat transfer media. As the general case, some oil is extracted from the tank and heated to a higher temperature in the heat exchanger. After that, the heated oil which is called hot oil will be pumped back to the tank and be sprayed by the nozzle to be mixed with the cold oil inside the tank. By the mixture process, the temperature of cold oil in the tank will be increased. In the tank, the nozzle and heating tube which is used to transform the hot oil become the main structure of this heating mode. Similar heating technologies are extensively applied in the heat supply system [1,2], but in essence, they belong to application of the jet flow technologies in the heat transfer field. Now the research references on this heating modes are relative limited, but research references on the jet flow based on the buoyancy formed by the heat spreading are plentiful. The early researchers include Jirka [3, 4], Lee [5] and Balasubramanian [6]. They mainly got the essential features of the phenomena such as

^{*} Correspondence to: Northeast Petroleum University, Fazhan Road No.199, Hi-tech Development Zone, Daqing 163318, China.
E-mail address: soulkissing@163.com (J. Zhao).

Nomenclature		Greek letters	
c_p	specific heat of crude oil, J/kg · °C	α	thermal diffusion coefficient of crude oil, m ² /s
D_j	nozzle diameter, m	α_t	turbulence thermal diffusion coefficient of crude oil, m ² /s
H_j	nozzle depth, m	ϕ	angle between the nozzle tangent and horizontal direction
p^*	static pressure, $p^* = p + 2/3\rho k$	η_j	temperature increase efficiency
$T(x, y, z)$	oil temperature, °C	κ_j	temperature distribution uniformity parameter
T_0	initial oil temperature inside the tank, °C	λ	heat conductivity of crude oil, W/m · K
T_j	spraying temperature, °C	μ	kinetic viscosity of crude oil, Pa · s
T_{bt}	temperature at the top wall, °C	μ_{eff}	effective viscosity coefficient, $\mu_{eff} = \mu + \mu_t$, $\mu_t = \rho C_\mu k^2/\varepsilon$
T_{bb}	temperature at the bottom wall, °C	ρ_a	density of fluid in the tank, kg/m ³
T_{bs}	temperature at the symmetry section, °C	ρ_j	density of spraying fluid, kg/m ³
T_{ave}	volume weighted average temperature in tank, °C	Indices/exponents	
T_{ave1}	average temperature in region 1, °C		
T_{ave2}	average temperature in region 2, °C	ave	average
T_{ave3}	average temperature in region 3, °C	a	oil in the tank
T_{ave4}	average temperature in region 4, °C	bt	top wall
T_{ave5}	average temperature in region 5, °C	bb	bottom wall
u_i, u_j	mean velocity u, v, w	bs	symmetry section
$u_0(x, y, z)$	initial velocity, m/s	j	Jet flow
$v_0(x, y, z)$	initial velocity, m/s	0	initial moment
$w_0(x, y, z)$	initial velocity, m/s	p	constant pressure
v_j	nozzle speed, m/s		
x_i	coordinate axis x, y, z		

vertical plane buoyancy jet flow and horizontal round buoyancy jet flow via the experimental methods. In recent years, the numerical simulation method is becoming a more effective method to solve these problems. Kuang [7,8] conducted numerical research on the plane vertical buoyancy jet flow by using the finite volume method and corrected $k - \varepsilon$ model. Wenxin [9] and Yuhong [10] deeply studied the stability and mixing features of buoyancy jet flow by using the numerical simulation method based on the hybrid finite analysis. All of above research took the water as the medium and are mainly belonged to the buoyancy jet flow problem under the shallow water environment in the hydrodynamics field. Although rich research achievements were achieved, the thermophysical property of crude oil is very different from that of water. Comparing to water, the viscosity of crude oil is much higher and more sensitive to the temperature. And the specific heat capacity of crude oil is about half of water. For the hot oil spraying heating process, the tank is the implemented place of buoyancy jet flow which is different from that in the existing literature as there is a limited space and greater depth. Even if the essential features are similar, existing research achievements can not be directly applied to the hot oil spraying heating process. As the numerical simulation method can cover different working conditions and get comprehensive data, it is used to investigate the hot oil spraying heating process in the crude oil tank so that the flow and heat transfer features during this heating process will be revealed which comes to be the foundation for adjustment and optimization of this heating mode.

2. Calculation model

2.1. Physical model

The research object is a floating roof oil tank which has a removable roof. So the oil can cling close to the roof. The interior zone with the nozzles and tube are taken as the simulated object. A photograph of the nozzle in the tank is shown in Fig. 1. There is always the same distance between two adjacent nozzles. So the tank can be divided into different parts based on the amount of nozzles. For each part, due to the symmetrical feature of structure, one half of the region where one nozzle occupies is taken as the computational domain. Fig. 2 illustrates the physical model and coordinate system of the computational domain. The height of the tank shown in Fig. 2 is 6 m, the radial length is 14 m. Fig. 3 is a separate sectional sketch which shows the detail of the nozzle structure. The diameter of the nozzle is 40 mm, and the angle between the nozzle and x-direction is 45 degree. As can be seen in Fig. 2, the symmetrical section which passes through the center of the nozzle is on the plane $z=0$. So the radial direction on the symmetrical section is parallel to the x-coordinate axis, while the axial direction of the tank is parallel to the y-coordinate axis.



Fig. 1. Photograph of nozzle.

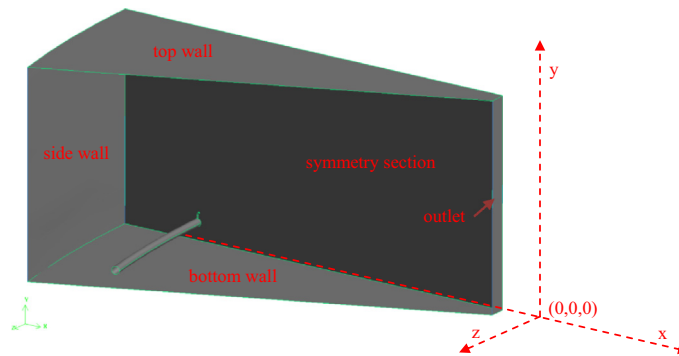


Fig. 2. Computational domain.

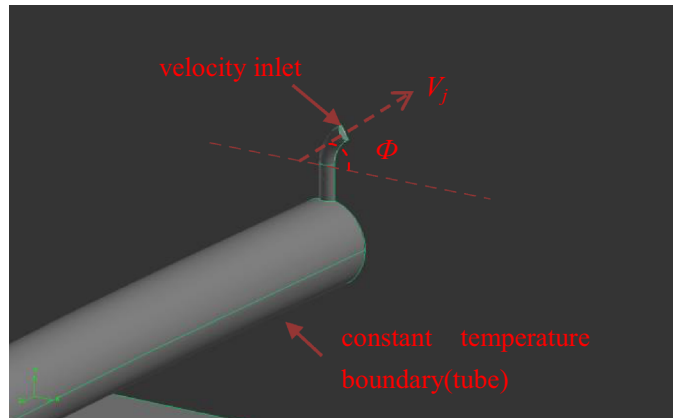


Fig. 3. Sectional sketch of nozzle.

2.2. Mathematic model

Based on the standard $k - \varepsilon$ model, the governing equations for the hot oil spraying heating process are shown as follows:

$$\text{Equation of Continuity } \frac{\partial \rho_a}{\partial t} + \frac{\partial (\rho_a u_i)}{\partial x_i} = 0 \quad (1)$$

$$\text{Momentum Equation } \frac{\partial(\rho_a u_i)}{\partial t} + \frac{\partial(\rho_a u_j u_i)}{\partial x_j} = -\frac{\partial p^*}{\partial x_i} + \frac{\partial \left[\mu_{\text{eff}} \left(\frac{\partial u_i}{\partial x_j} + \frac{\partial u_j}{\partial x_i} \right) \right]}{\partial x_j} \quad (2)$$

$$\text{Energy Equation } \frac{\partial(\rho_a T)}{\partial t} + \frac{\partial(\rho_a u_i T)}{\partial x_i} = \frac{\partial}{\partial x_i} \left[\rho_a \left(\alpha + \frac{\alpha_t}{\sigma_t} \right) \frac{\partial T}{\partial x_i} \right] \quad (3)$$

$$\text{Turbulence } k \text{ Equation } \frac{\partial(\rho_a k)}{\partial t} + \frac{\partial}{\partial x_j} \left[\rho_a u_j k - \left(\mu + \frac{\mu_t}{\sigma_k} \right) \frac{\partial k}{\partial x_j} \right] = \rho_a (p_k - \epsilon) \quad (4)$$

$$\text{Turbulence } \epsilon \text{ Equation } \frac{\partial(\rho_a \epsilon)}{\partial t} + \frac{\partial}{\partial x_j} \left[\rho_a u_j \epsilon - \left(\mu + \frac{\mu_t}{\sigma_\epsilon} \right) \frac{\partial \epsilon}{\partial x_j} \right] = \rho_a \frac{\epsilon}{k} (C_{\epsilon 1} p_k - C_{\epsilon 2} \epsilon) \quad (5)$$

where,

$$p_k = \frac{\mu_t}{\rho_a} \left(\frac{\partial u_i}{\partial x_j} + \frac{\partial u_j}{\partial x_i} \right) \frac{\partial u_i}{\partial x_j} \quad C_\mu = 0.09 \quad C_{\epsilon 1} = 1.44 \quad C_{\epsilon 2} = 1.92 \quad \sigma_k = 1.0 \quad \sigma_\epsilon = 1.3 \quad (6)$$

The simulated crude oil is from Da Qing oil field. The basic physical property equations are shown as follows:

$$\text{Kinetic Viscosity } \mu: \begin{cases} T > 40^\circ\text{C}, \mu = 0.00002T^2 - 0.00211T + 0.08162 \\ T \leq 40^\circ\text{C}, \mu = -0.0001T^4 - 0.0212T^3 + 1.1759T^2 - 28.9773T + 267.8962 \end{cases} \quad (7)$$

$$\text{Specific Heat } c_p: \begin{cases} T > 50^\circ\text{C}, c_p = 2.185T + 1912.3 \\ T \leq 50^\circ\text{C}, c_p = -31.479T + 3612.7 \end{cases} \quad (8)$$

$$\text{Heat Conductivity } k_a: k_a = 0.137 \cdot \frac{1 - 0.00054T}{0.856} \quad (9)$$

$$\text{Density } \rho_a: \rho_a = 850 \cdot [1 - 0.000844(T - 20)] \quad (10)$$

Boundary conditions:

Velocity inlet: $u = v_j \cos \phi$, $v = v_j \sin \phi$, $w = 0$, $T = T_j$, $k = 0.06v_j^2$, $\epsilon = 0.06 \frac{v_j^3}{D}$.

Top wall: $u = v = w = 0$, $-k_a \frac{\partial T_{\text{bt}}}{\partial y} = 0$, k and ϵ are solved by the standard wall function.

Bottom wall: $u = v = w = 0$, $-k_a \frac{\partial T_{\text{bb}}}{\partial y} = 0$, k and ϵ are solved by the standard wall function.

Outlet: $\frac{\partial u}{\partial x} = \frac{\partial v}{\partial x} = \frac{\partial w}{\partial x} = \frac{\partial k}{\partial x} = \frac{\partial \epsilon}{\partial x} = \frac{\partial T}{\partial x} = 0$.

Symmetry boundary: $w = 0$, $-k_a \frac{\partial T_{\text{bs}}}{\partial y} = 0$.

Initial condition: $T(x, y, z) = T_0$, $u_0(x, y, z) = v_0(x, y, z) = w_0(x, y, z) = 0$.

2.3. Numerical solving method

In order to improve the quality of the mesh, the computational domain is divided into different blocks. The nozzle area is the non-structural tetrahedron mesh and the mesh is encrypted. The structural hexahedron mesh is used outside this area. The mesh deployment is disperse. the finally total mesh unit number can approximate to 500,000. The finite volume method is used for the control equation discretion. The central differencing scheme is used for diffusion terms. The improved QUICK format is used for convection item [11]. The implicit time discretisation scheme is used for time discretion. The PISO algorithm suitable for solving the instantaneous state problem is used to solve the control equations.

3. Simulation results and analysis

24 computing conditions are designed, the parameter of different conditions is shown in table1. For all the 24 computing conditions, the diameter of nozzle is 0.04 m. The angle of the nozzle is 45 degree. The initial temperature of oil in the tank is 36 °C. According to the research on buoyancy jet from Jirka [3], Froude number and relative submersion depth δ is defined as follows:

$$\text{Fr} = \frac{v_j}{\sqrt{(\rho_a - \rho_j)gD_j/\rho_a}} \quad (11)$$

$$\delta = \frac{H_j}{D_j} \quad (12)$$

The mathematic models were solved following the method shown in 2.3. Except for case 1, case 7, case 13 and case 19, other cases have been done with the standard k-eps turbulence model. Case 1, case 7, case 13 and case 19 were deal as the laminar flow. Based on the feature of temperature and velocity profile, the type of hot oil spraying heating mode is divided

Table 1
Parameter of simulating conditions.

Number of run	Diameter (m)	Tank level (m)	Nozzle speed (m/s)	Spraying temperature (°C)	Reynolds-Number	Froude Number	Relative submersion depth
1	28.5	6	0.4	75	1650	15.6	130.8
2	28.5	6	1.73	75	7136	67.4	130.8
3	28.5	6	3.5	81	14,425	118.1	130.8
4	28.5	6	3.5	75	14,437	136.3	130.8
5	28.5	6	3.5	50	8963	379.6	130.8
6	28.5	6	5.57	50	14,265	604.1	130.8
7	28.5	10	0.4	75	1650	15.6	230.8
8	28.5	10	3.5	81	14,425	118.1	230.8
9	28.5	10	3.5	50	8963	379.6	230.8
10	28.5	10	11.1	57	36,598	799.6	230.8
11	28.5	10	6.91	48	16,385	874.3	230.8
12	28.5	10	11.1	50	28,427	1199.4	230.8
13	60	6	0.4	75	1650	15.6	130.8
14	60	6	1.73	75	7136	67.4	130.8
15	60	6	3.5	81	14,425	118.1	130.8
16	60	6	3.5	75	14,437	136.3	130.8
17	60	6	3.5	50	8963	379.6	130.8
18	60	6	5.57	50	14,265	604.1	130.8
19	60	10	0.4	75	1650	15.6	230.8
20	60	10	3.5	81	14,425	118.1	230.8
21	60	10	3.5	50	8963	379.6	230.8
22	60	10	11.1	57	36,598	799.6	230.8
23	60	10	6.91	48	16,385	874.3	230.8
24	60	10	11.1	50	28,427	1199.4	230.8

into the strong buoyancy process, weak buoyancy process and normal buoyancy process.

3.1. Strong buoyancy process

For the first case in Table 1, the nozzle speed is 0.4 m/s, while the spraying temperature is 75 °C. The corresponding Froude number is 15.6 which is far less than the relative submission depth of 130.8. In this case, the formed jet flow features the strong buoyancy and weak initial moment. The temperature field profile at different times on the symmetry section is shown in Fig. 4. Fig. 5 shows the temperature field profile of the section on plane $X = -11$ which exits perpendicular to the symmetry section.

Under this state, the jet flow formed by the hot oil spraying has small initial moment and strong buoyancy. The jet flow only sprays in the tangent direction of the nozzle in close distance from the nozzle and then moves in the direction quasi-perpendicular to the tank top under the action of the buoyancy. The jet flow entrains the surrounding crude oil and increases its temperature by mixing with it. With this process proceeding, the jet flow speed reduces and the outer limit of the jet flow gradually expands. When the jet flow contacts the tank roof, it spreads along the wall surface taking the touch point as the center and the oil temperature inside the tank will increase from up to down layer by layer. On this condition, the oil temperature at the passing path of the jet flow is high. On the whole, the oil temperature in the tank has layering distribution in the axial direction. The temperature of oil close to the tank roof is higher. Except for the passing path of the jet flow, the oil temperatures at same heights are similar. In order to investigate the axial temperature distribution characteristic, different radial positions are picked which is shown in Fig. 6. The axial temperature distribution as a function of time at different radial positions on the symmetry section is shown in Figs. 7–10. The essential features of temperature field obtained by the numerical computing are roughly consistent with that from Jirka [3] and Kuang [8] via experimental and

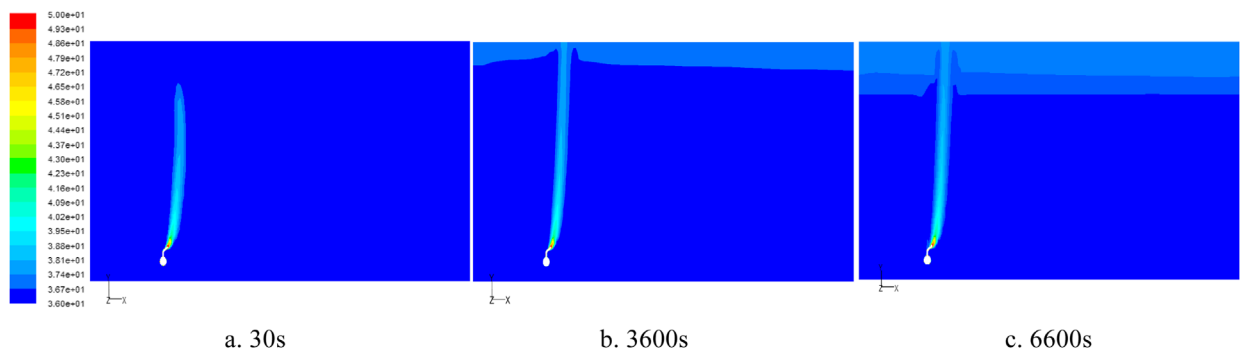


Fig. 4. Temperature field profile of symmetry section.

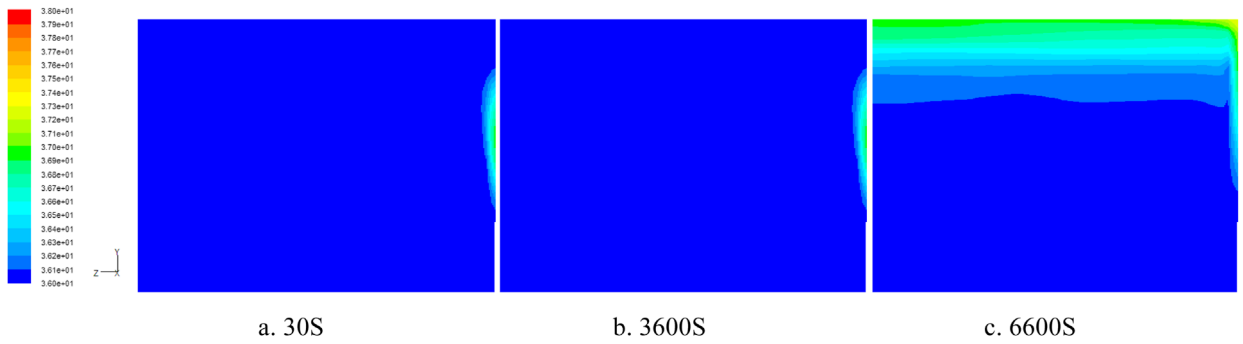


Fig. 5. Temperature field profile of section on plane $X = -11$.

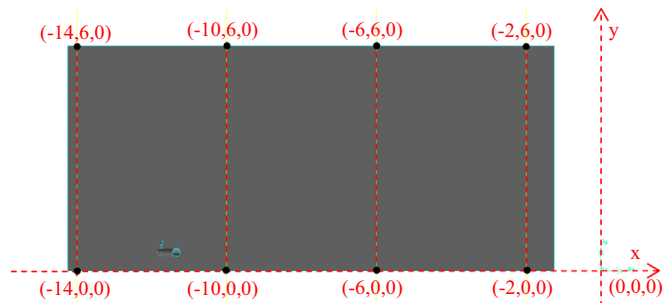


Fig. 6. Sectional sketch of symmetry section.

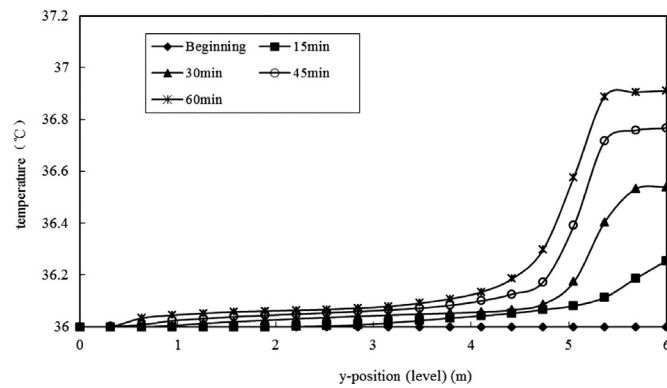


Fig. 7. Temperature distribution at $X = -2$ at different times.

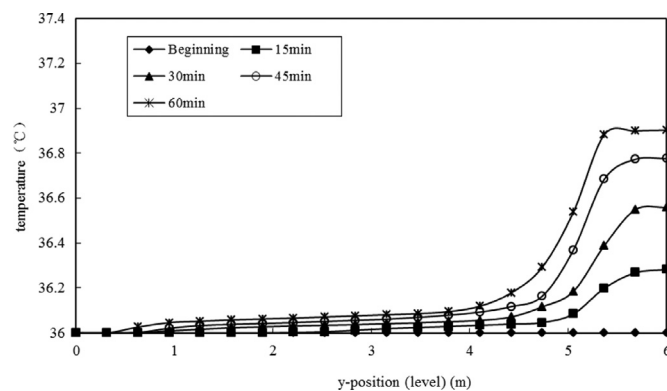


Fig. 8. Temperature distribution at $X = -6$ at different times.

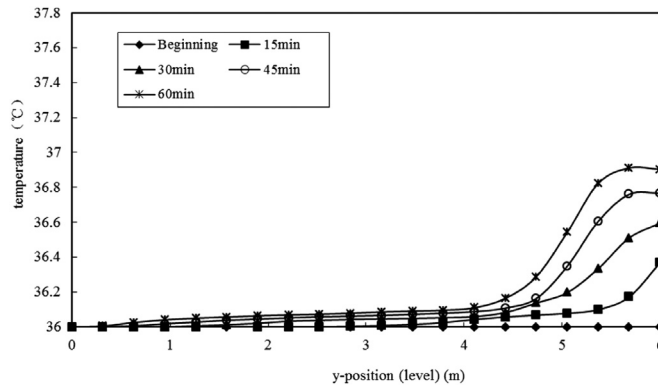


Fig. 9. Temperature distribution at $X = -10$ at different times.

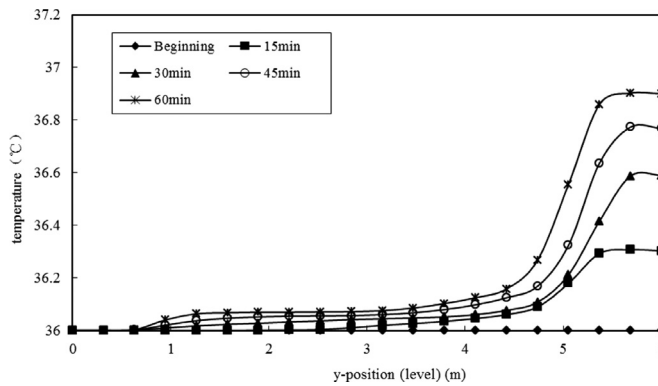


Fig. 10. Temperature distribution at $X = -14$ at different times.

numerical simulation when the water buoyancy jet flow is stably discharged. At this time, due to the stronger buoyancy and weaker initial moment, the cold and hot oil inside the tank hardly get sufficient mix, the oil temperature distribution is not so uniform. At the bottom of the tank, especially the region below the nozzle and tube turns into the dead heating area.

3.2. Weak buoyancy process

For the sixth case in Table 1, the nozzle speed is 5.57 m/s, while the spraying temperature is 50 °C. The corresponding Froude Number is 604.1 which is far higher than the relative submission depth of 130.8. At this time, the formed jet flow features the strong initial moment and weak buoyancy. The temperature field profile of symmetry section and the section on plane $X = -11$ is shown in Fig. 11 and 12. On this condition, the jet flow formed by the hot oil spraying can spray longer distance along the nozzle tangent direction under the initial moment. It will entrain the surrounding fluid and increase its temperature. The jet flow has stronger initial moment. After it contacts the tank roof, the jet flow will lead to rotation of the fluid within certain range, form stronger heat exchange and drive uniform distribution of the oil temperature at certain height. Figs. 13–16 lists the axial temperature distribution as a function of time at different radial positions on the symmetry

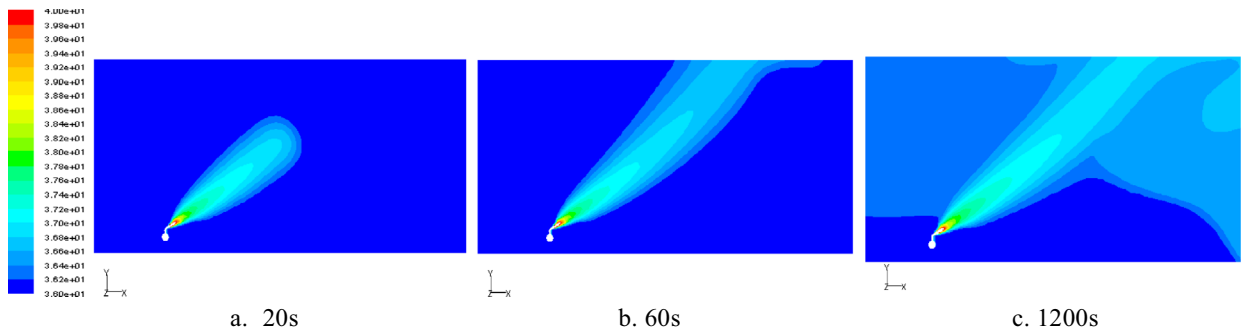


Fig. 11. Temperature field profile of symmetry section.

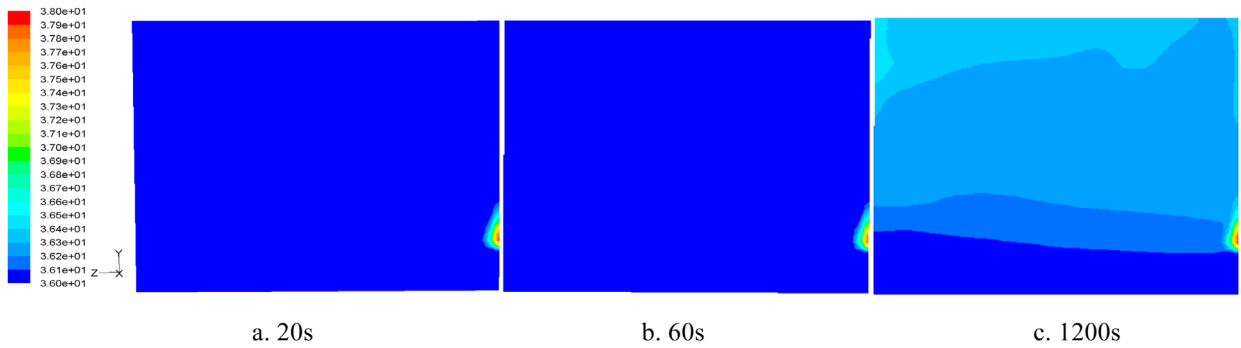


Fig. 12. Temperature field profile of section on plane $X = -11$.

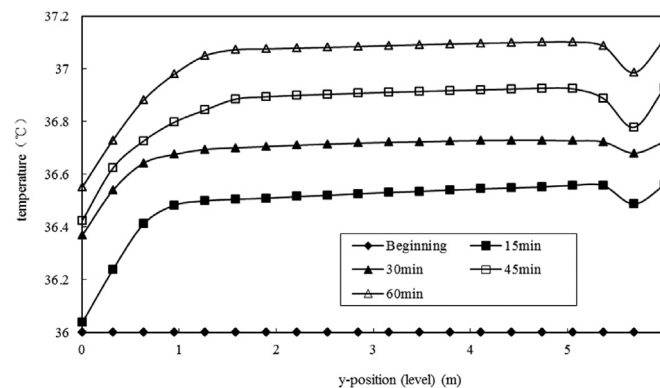


Fig. 13. Temperature distribution at $X = -2$ at different times.

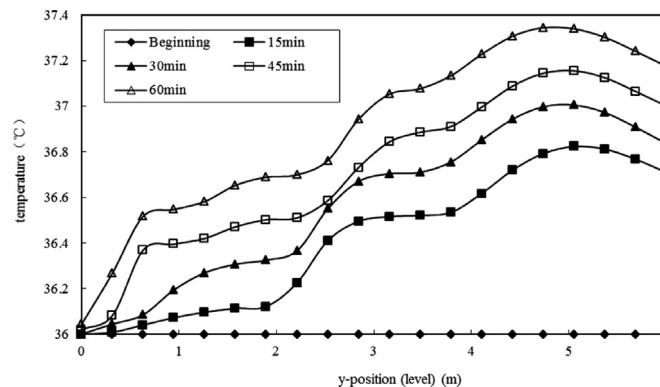


Fig. 14. Temperature distribution at $X = -6$ at different times.

section. Comparing to the strong buoyancy process, on this condition, the crude oil at high-level can generate stronger heat exchange. The axial temperature difference decreases with the oil temperature distribution more uniform. However, the temperature of oil close to the tank bottom is still low. The essential features of temperature field obtained by the numerical computing are roughly consistent with that obtained by Jirka [3] and Kuang [8] via experimental and numerical simulation when the water buoyancy jet flow is stably discharged.

3.3. Influence of Froude Number on effect of hot oil spraying heating

To evaluate the heating effect of the hot oil spraying inside the tank, two parameters including “temperature increase efficiency” and “temperature distribution uniformity” are defined as the evaluation indices. The “temperature increase efficiency” is defined as follows:

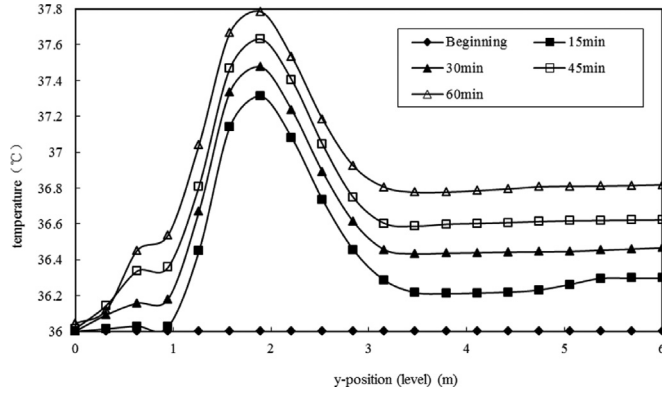


Fig. 15. Temperature distribution at $X = -10$ at different times.

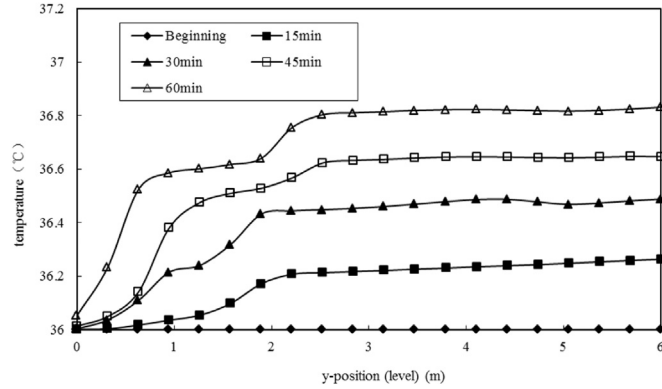


Fig. 16. Temperature distribution at $X = -14$ at different times.

$$\eta_j = \frac{(T_{ave} - T_0)}{(T_j - T_0)} \times 100\% \quad (13)$$

The spraying temperature of the hot oil spraying can represent the extreme temperature of the heated crude oil. The temperature increase efficiency can represent the percent of average oil temperature increase ($T_{ave} - T_0$) to the extreme temperature increase ($T_j - T_0$) inside the tank at any time. Larger value of η_j indicates that the jet flow is mixed well with the cold oil inside the tank and the utilization rate of the jet flow temperature is higher. The “temperature increase efficiency” as a function of heating time at different Froude Number is shown in Fig. 17. The calculated results are extracted from case 6 ($Fr=604$), case 3 ($Fr=118$) and case 2 ($Fr=67$). From this figure, bigger Froude Number brings a weak buoyancy process so that the jet flow can be mixed better with the cold oil inside the tank. Smaller Froude Number indicates a strong buoyancy

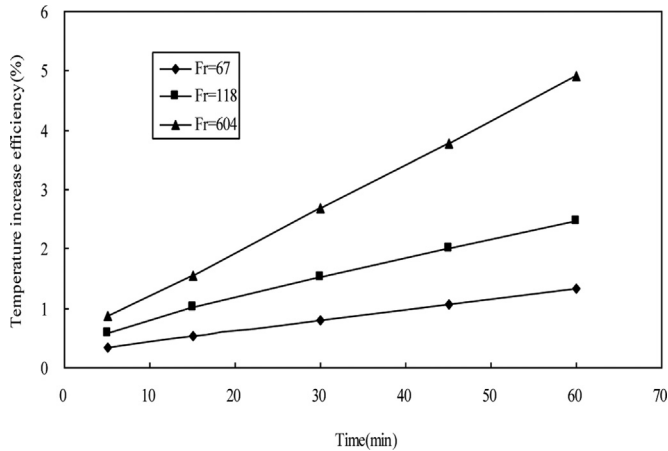


Fig. 17. “Temperature increase efficiency” as a function of time at different Froude Number.

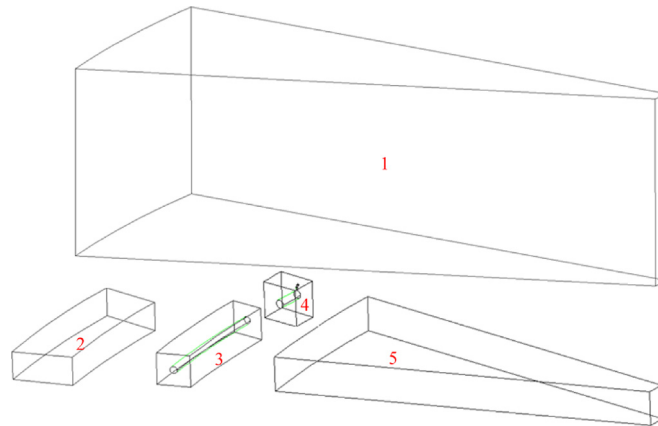


Fig. 18. Division of computational domain.

process. Between them is the common buoyancy process. If the heating rate is taken as concern, bigger Froude Number brings a better heating effect. Longer heating time indicates higher temperature increase efficiency of the crude oil. When the hot oil spraying heating method is used, Froude Numbers should be referred and the spraying temperature and nozzle speed should be controlled. Only increasing the temperature can not ensure quick increase of the oil temperature. Higher nozzle speed can drive quick spreading of the jet flow.

In order to investigate the temperature distribution uniformity, the tank is divided into five parts. The partition of different region is shown in Fig. 18. During the heating process, different regions get different influence from the heating nozzle and tube. Region 3 and region 4 include the nozzle and heating tube, the temperature of which is much higher than that of the other regions. Region 2 and region 5 exiting at the bottom of the tank are always deemed to be the dead zone which is least affected from the hot oil spraying heating. Region 1 exiting on the top of the nozzle is the main region of the tank. Larger temperature deviation among different regions reflects more uneven temperature distribution. On another perspective, the temperature distribution uniformity parameter inside the tank is defined to reflect the heating effect under the hot oil spraying heating mode:

$$\kappa_j = \frac{\text{Max}(T_{\text{ave}1}, T_{\text{ave}2}, T_{\text{ave}3}, T_{\text{ave}4}, T_{\text{ave}5}) - \text{Min}(T_{\text{ave}1}, T_{\text{ave}2}, T_{\text{ave}3}, T_{\text{ave}4}, T_{\text{ave}5})}{T_{\text{ave}}} \times 100\% \quad (14)$$

According to the simulated result from different cases in Table 1, the changing rule of oil temperature distribution non-uniformity inside the tank is obtained. The simulated result from case 3 ($Fr = 118$), case 4 ($Fr = 136$), case 5 ($Fr = 380$) and case 6 ($Fr = 604$) are shown in Fig. 19.

In Fig. 19, the x-axis represents the average temperature of oil inside the tank, the “non-uniformity of temperature distribution” is taken as the Y-axis. When the heating is proceeding, the average temperature of oil inside the tank increases, together with the “non-uniformity of temperature distribution”. In Fig. 19, for the given case, with the heating time going, the average oil temperature increases, together with the temperature distribution non-uniformity. For different cases, at the same average temperature, a case with bigger Froude Number indicates stronger initial moment, weaker buoyancy, so that a stronger heat exchange between cold and hot oil and more uniform mixing of oil temperature arises. When the nozzle speed

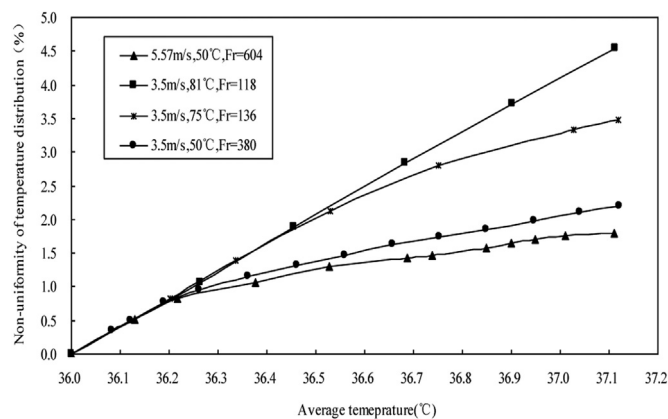


Fig. 19. “Non-uniformity of temperature distribution” as a function of average temperature at different Froude Number.

reduces and the spraying temperature increases, the buoyancy becomes stronger, the axial layering distribution feature of temperature inside the tank is more significant, heat exchange between cold and hot oil becomes weak, the temperature uniformity becomes worse. In addition, the average oil temperature will increase and non-uniformity of the oil temperature distribution will be slowly enhanced with heating progress.

4. Conclusions

- (1) The numerical simulating model of the hot oil spraying heating process in the floating roof oil tank was established. Based on the finite volume method and standard $k - \varepsilon$ turbulence model, numerical simulations for heating process under different parameters were performed. The results indicate that this heating mode has the similar features with buoyancy jet flow. The distribution of oil temperature is affected by Froude Number and relative submission depth. The strong buoyancy, weak buoyancy and common buoyancy are divided.
- (2) Bigger Froude Number indicates weaker buoyancy and stronger initial moment. On this condition, the heat exchange is more intense and the oil temperature distribution becomes more uniform. Higher temperature increase efficiency and temperature increase rate heating arises. On the contrary, smaller Froude Number indicates stronger buoyancy and weaker initial moment. The axial layering distribution feature of oil temperature becomes more significant and the heat exchange effect is weaker.
- (3) The nozzle speed and spraying temperature should be adjusted synchronously based on Froude Number during practical usage of hot oil spraying heating mode. In order to improve the effect of the hot oil spraying heating process, the spraying flow rate should be as high as possible, but the spraying temperature should not be too high.

Conflict of interest

Financial contributions to the work being reported should be clearly acknowledged, as should any potential conflict of interest.

There is no conflict of interest.

Acknowledgments

This paper is supported by PetroChina Innovation Foundation (2014D-5006-0607).

This paper is supported by Youth Fund of Northeast Petroleum University.

References

- [1] G. Yang, Application and energy saving of jet mixing heat in heat supply system, *Energy Sav. Environ. Prot.* 8 (2006) 41–44.
- [2] Z. Kun, C. Zhiguang, H. Xiang, Application of automatically controlled jet heat exchanger in heat supply system, *Area Heat Supply* 4 (2010) 72–74.
- [3] G.H. Jirka, D.R.F. Harleman, Stability and mixing of vertical Plane buoyant jet in confined depth, *J. Fluid Mech.* 2 (1979) 275–304.
- [4] G.H. Jirka, Multiport diffusers for heat disposal: a summary, *J. Hydraul. Div.* 12 (1982) 1425–1486.
- [5] J.H.W. Lee, G.H. Jirka, Vertical round buoyant jet in shallow water, *J. Hydraul. Div.*, 12, ASCE (1981), pp. , 1981, 1651–1675.
- [6] V. Balasubramanian, C. Subhashjain, Horizontal buoyant jets in quiescent shallow water, *J. Environ. Eng. Div.* 4 (1978) 717–729.
- [7] C.P. Kuang, J.H.W. Lee, A numerical study on the stability of a vertical Plane jet in confined depth, in: *Proceeding of the 2nd International Symposium on Environmental Hydraulics*, 1998, pp. 205–210.
- [8] C.P. Kuang, J.H.W. Lee, Effect of downstream control on stability and mixing of a vertical buoyant jet in confined depth, *J. Hydraul. Res.* 4 (2001) 165–174.
- [9] H. Wenxin, Jet flow rolling Flow and buoyance Jet Flow under Static Environment, Doctor Dissertation of Wuhan University, 1991.
- [10] Z. Yuhong, Research on buoyance Jet Flow Stability and mixing Feature under Static Shallow Water Environment, Doctor Dissertation of Wuhan University, 2005.
- [11] T. Hayase, J.A.C. Humphrey, R. Greif, A consistently formulated QUICK scheme for fast and stable convergence using finite-volume iterative calculation procedures, *J. Comput. Phys.* 98 (1992) 108–118.